DOI: 10.24850/j-tyca-2026-01-08

Articles

Hydraulic performance optimization of triangular-arced asymmetric labyrinth weirs: Experimental analysis of discharge efficiency and geometric variations

Optimización del comportamiento hidráulico de vertederos laberínticos asimétricos con arcos triangulares: análisis experimental de la eficiencia de descarga y variaciones geométricas

Seyed Mohammad Tabatabai[1], ORCID: https://orcid.org/0000-0003-2829-8278

Mohammad Heidranejad[2], ORCID: https://orcid.org/0000-0002-7306-3614

Alireza Masjedi[3], ORCID: https://orcid.org/0000-0002-2953-3519

Amin Bordbar[4], ORCID: https://orcid.org/0000-0001-7632-5766

[1]Department of Water Science Engineering, Ahvaz Branch, Islamic Azad University, Ahvaz, Iran, mohammad_pilot2009@yahoo.com

[2]Department of Water Science Engineering, Ahvaz Branch, Islamic Azad University, Ahvaz, Iran, mo_he3197@yahoo.com

[3]Department of Water Science Engineering, Ahvaz Branch, Islamic Azad University, Ahvaz, Iran, drmasjedi.2007@yahoo.com

2026, Instituto Mexicano de Tecnología del Agua. Open Access bajo la licencia CC BY-NC-SA 4.0 (https://creativecommons.org/licenses/by-nc-sa/4.0/)

[4]Department of Water Science Engineering, Ahvaz Branch, Islamic Azad University, Ahvaz, Iran, asefmn@yahoo.com

Corresponding author: Mohammad Heidarnejad, mo_he3197@yahoo.com

Abstract

This study examines the hydraulic performance of triangular-arced asymmetric labyrinth weirs with varying middle cycles, focusing on optimizing the discharge coefficient (Cd) under different geometric and hydraulic conditions. Experimental investigations were conducted in a flume with triangular-arced weirs featuring arc angles of 45°, 90°, and 135°. The results indicate that the highest Cd of 0.949 was achieved at a Froude number (Fr) of 1.64 and an arc angle of 90°, demonstrating optimal hydraulic performance. Wider intermediate cycles (R/W1 = 3.2) enhanced Cd to 0.949, while narrower cycles (R/W1 = 2.5) yielded a lower Cd of 0.633 due to increased turbulence and flow interference. The Q-Ht curves revealed that reducing the apex width (W1) increased upstream hydraulic head, enhancing discharge coefficient at low discharges but reducing hydraulic efficiency at higher discharges due to turbulence. These findings confirm that modifying intermediate cycles and optimizing arc angles can significantly improve hydraulic efficiency.

Keywords: Labyrinth weir, triangular plan weir, PKW, discharge coefficient.

2026, Instituto Mexicano de Tecnología del Agua.
Open Access bajo la licencia CC BY-NC-SA 4.0
(https://creativecommons.org/licenses/by-nc-sa/4.0/)

Resumen

Este estudio examina el rendimiento hidráulico de vertederos laberínticos asimétricos con arcos triangulares y ciclos intermedios variables, centrándose en la optimización del coeficiente de descarga (Cd) bajo diferentes condiciones geométricas e hidráulicas. Se llevaron a cabo investigaciones experimentales en un canal con vertederos de arcos triangulares que presentaban ángulos de arco de 45°, 90° y 135°. Los resultados indican que el Cd más alto, de 0.949, se logró a un número de Froude (Fr) de 1.64 y un ángulo de arco de 90°, lo que demostró un rendimiento hidráulico óptimo. Los ciclos intermedios más anchos (R/W1 = 3.2) mejoraron el Cd a 0.949, mientras que los ciclos más estrechos (R/W1 = 2.5) produjeron un Cd más bajo de 0.633 debido al aumento de la turbulencia y la interferencia del flujo. Las curvas Q-Ht revelaron que la reducción del ancho del morro (W1) incrementó los niveles de agua aguas arriba y mejoró la descarga a bajos caudales, pero redujo la eficiencia a descargas más altas debido a la turbulencia. Estos hallazgos confirman que la modificación de los ciclos intermedios y la optimización de los ángulos de arco pueden mejorar significativamente la eficiencia hidráulica.

Palabras clave: vertedero laberíntico, vertedero de plano triangular, PKW, coeficiente de descarga.

Received: 06/03/2025

Accepted: 17/05/2025

Available ahead of print: 03/06/2025

Version of record: 01/01/2026

2026, Instituto Mexicano de Tecnología del Agua. Open Access bajo la licencia CC BY-NC-SA 4.0 (https://creativecommons.org/licenses/by-nc-sa/4.0/)

Tecnología y Ciencias del Agua
OPEN ACCESS
Check for updates

Introduction

Labyrinth weirs are a suitable solution for locations where width is limited. Featuring a non-linear crest, these weirs offer a longer crest length compared to straight-crested weirs of the same width. Consequently, under equivalent hydraulic head conditions, they can accommodate a greater discharge. Due to their capacity to handle high discharges with relatively low hydraulic heads, labyrinth weirs require less space in the design layout, making them a cost-efficient option for various applications (Hashem, Mohammed, & Alfatlawi, 2024; Zhu, Si, Xie, & Tan, 2024; Seyedian, Haghiabi, & Parsaie, 2023; Wang, Zheng, Ren, Liu, & Wu, 2022; Majedi-Asl, Fuladipanah, Arun, & Tripathi, 2022). Figure 1 shows the geometric and hydraulic parameters of a triangular and trapezoidal labyrinth weir plan. Figure 2 shows the layout of the arched weir used as the control sample.

2026, Instituto Mexicano de Tecnología del Agua.
Open Access bajo la licencia CC BY-NC-SA 4.0
(https://creativecommons.org/licenses/by-nc-sa/4.0/)

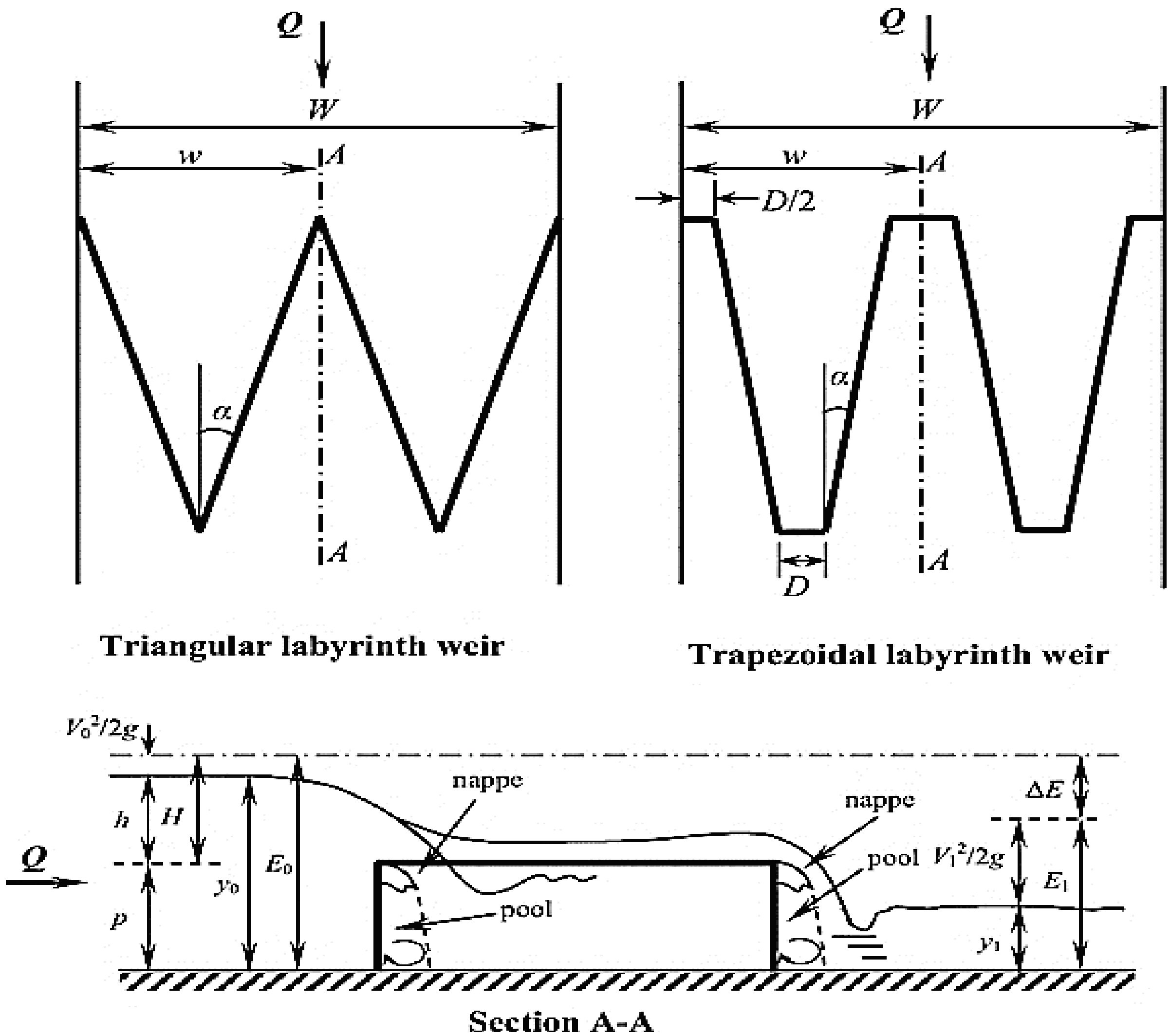

Figure 1. Geometric and hydraulic parameters of triangular and trapezoidal labyrinth weir plan.

2026, Instituto Mexicano de Tecnología del Agua. Open Access bajo la licencia CC BY-NC-SA 4.0 (https://creativecommons.org/licenses/by-nc-sa/4.0/)

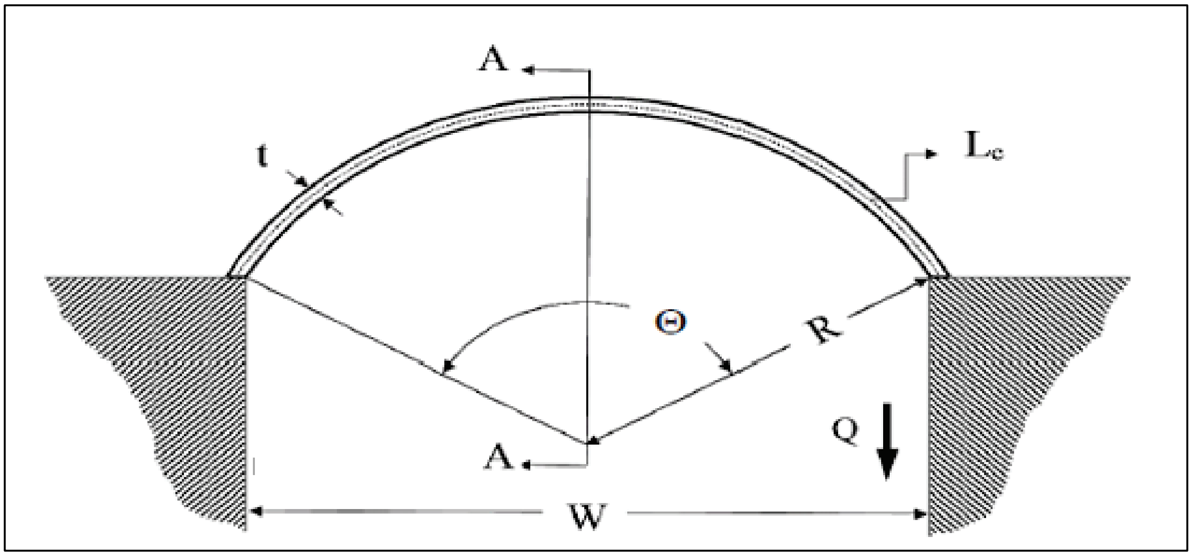

Figure 2. A plan and section view of arced weir.

In Figure 1, Q is the discharge, w is the labyrinth weir cycle width, P is the weir height, α is the sidewall angle (crest), D is the width of the weir apex and W is the total width of the weir.

The parameters listed in the Figure 2 are defined as follows:

$V^2/2g$ = Velocity head, representing the kinetic energy of the fluid expressed in terms of height (V: Velocity of the fluid, g: Acceleration due to gravity)

h = Hydraulic head (e.g., the free surface elevation from a reference point)

H_0 = Total hydraulic head, which is the sum of the velocity head, pressure head, and elevation head

Q = Discharge (volumetric discharge of the fluid per unit time)

P = Height weir

L_0 = Total weir length

2026, Instituto Mexicano de Tecnología del Agua. Open Access bajo la licencia CC BY-NC-SA 4.0 (https://creativecommons.org/licenses/by-nc-sa/4.0/)

Tecnología y ciencias del agua, ISSN 2007-2422, 17(1), 314-348. DOI: 10.24850/j-tyca-2026-01-08

W = Total width of a section (depending on context)

D = Hydraulic head in the downstream of weir

Labyrinth weirs have garnered significant attention for their hydraulic efficiency, particularly in flood control and spillway design. Early studies, such as those by Taylor (1968), and Hay and Taylor (1970), focused on sharp-edged crests with trapezoidal and triangular configurations. Darvas (1971) found that discharge coefficients decrease with increasing hydraulic head and increase with weir length. Subsequent research by Cassidy, Gardner and Peacock (1985) showed lower efficiency than previously expected, and Falvey (2003) identified key performance variables, such as total head-to-weir height ratio and sidewall angle. Ghare, Mhaisalkar and Porey (2008) used regression analysis to develop an empirical model for discharge coefficient optimization. Further studies by Khode, Tembhurkar, Porey and Ingle (2011) revealed the relationship between discharge coefficient and the H/P ratio, noting that sidewall angle affected flow and discharge. Anderson and Tullis (2011) investigated various geometries of piano key weirs and demonstrated that the discharge coefficient increases with the ratio of Wi/Wo (Inlet cycle width to outlet cycle width). They recommended an optimal range for this ratio between 1.25 and 1.5. Additionally, they emphasized that the upstream and downstream slopes, along with the installation of the apex, contribute to enhancing the efficiency of the weir. Kumar, Ahmad, Mansoor and Himanshu (2012) focused on sharp-crested curves under free-flow conditions, while Mirnaseri and Emadi (2014) examined the effects of weir length, height, and flume bed slopes on discharge coefficients. Gupta, Kumar and Ahmad (2015) compared rectangular labyrinth weirs with conventional weirs, finding improved discharge efficiency. Monjezi, Heidarnejad, Masjedi, Purmohammadi and Kamanbedast (2018) noted

2026, Instituto Mexicano de Tecnología del Agua. Open Access bajo la licencia CC BY-NC-SA 4.0 (https://creativecommons.org/licenses/by-nc-sa/4.0/)

that hydraulic headincreases caused a standing wave downstream, reducing the efficiency of arced-triangle labyrinth weirs. Azimi and Hakim (2019) showed that approach velocity and pool aspect ratio influence discharge coefficients and proposed semi-empirical formulas to predict discharge. Dizabadi, Hakim and Azimi (2020) introduced a new design featuring a square pool at the vertex, which extended the weir length and improved efficiency. Le, Hiramatsu and Nishiyama (2021) explored the use of computational fluid dynamics (CFD) to study the discharge capacity of piano key and rectangular labyrinth weirs, highlighting the inefficiency of physical model tests alone. Their findings indicate that the piano key weir outperforms the rectangular labyrinth weir, particularly due to higher sidewall discharge efficiency. Dehghani and Varaki (2021) studied the effects of upstream sedimentation (0 to 90% of weir height) and downstream bed levels on trapezoidal labyrinth weirs. They found that sedimentation up to 60% had minimal impact on discharge coefficients, while higher sedimentation reduced efficiency. Tailwater levels also influenced flow patterns, leading to statistical equations for discharge coefficient estimation. Namazi and Mozaffari (2023) found triangular labyrinth weirs to be more efficient than semicircular ones. Increasing total head ratio and weir cycles reduced efficiency due to nappe interference. Mattos-Villarroel *et al*. (2023) emphasized the suitability of labyrinth weirs for spillway design and dam safety, using Computational Fluid Dynamics (CFD) for discharge analysis. Ben-Said, Hafnaoui and Madi (2023) highlighted the influence of channel bed levels, revealing that lowering downstream beds increased discharge capacity by reducing submergence effects. Recent studies by Masoudi, Yari, Sadeghian and Norouzi (2024) showed that varying crest lengths significantly improved discharge coefficients by 40.7 and 35.3% for rectangular and trapezoidal

2026, Instituto Mexicano de Tecnología del Agua.
Open Access bajo la licencia CC BY-NC-SA 4.0
(https://creativecommons.org/licenses/by-nc-sa/4.0/)

weirs, respectively. Aydin, Ulu and Işık (2024) identified the importance of flow conditions in upstream and downstream cycles for hydraulic efficiency. Said and Ouamane (2024) explored modifications in overhang configurations, finding that these improvements enhanced labyrinth weir performance.

The objective of the present study is to investigate the discharge coefficient of a triangular-arched asymmetrical labyrinth weir with a widened middle cycle. The arched shape in the plan a higher discharge coefficient, which is the main focus of this study. Based on previous research, no comprehensive studies have been conducted on this topic. Also the primary aim of this study is to analyze variations in Cd of an asymmetric arched weir with a triangular cross-section.

Materials and methods

Experimental test

The study examines the influence of the arch angle and, consequently, the weir length on the discharge coefficient. Figure 3 provides an example of a labyrinth weir with an asymmetric triangular cross-section. Figure 4 presents the experimental flume, the labyrinth weirs, and a schematic representation of the laboratory setup employed in this research. Figure 5 depicts the weirs utilized during the experimental procedures. The experimental investigation was carried out in the hydraulic laboratory of the Khuzestan Water and Power Authority, Iran. The weir models were positioned within a testing flume measuring 8 meters in length, 0.6 meters in width, and 0.6 meters in height. The flume, constructed with transparent Plexiglas walls, enabled clear observation of water surface

2026, Instituto Mexicano de Tecnología del Agua. Open Access bajo la licencia CC BY-NC-SA 4.0 (https://creativecommons.org/licenses/by-nc-sa/4.0/)

profiles and flow behavior. It operated under free-flow conditions and was meticulously designed to be both watertight and seamless to ensure accurate results. The experimental setup included several components: a groundwater tank, a digital flowmeter with a precision of 0.2 l/s, a tranquilizer, a floating electric pump with a maximum discharge of 140 m^3/h, and a constant-head tank. The flume's base was a fixed-bed type and was carefully maintained in a horizontal orientation. Water was pumped from the groundwater tank into the head tank, from which it flowed through a 0.3-meter diameter pipe into the flume's inlet, controlled by a globe valve. At a low discharge, water entered the flume and passed smoothly over the weir. By adjusting the discharge, data on hydraulic conditions upstream, across, and downstream of the weir were recorded. Finally, flow exited the flume into a downstream channel, flowed into the pumping tank, and was subsequently recirculated into the system.

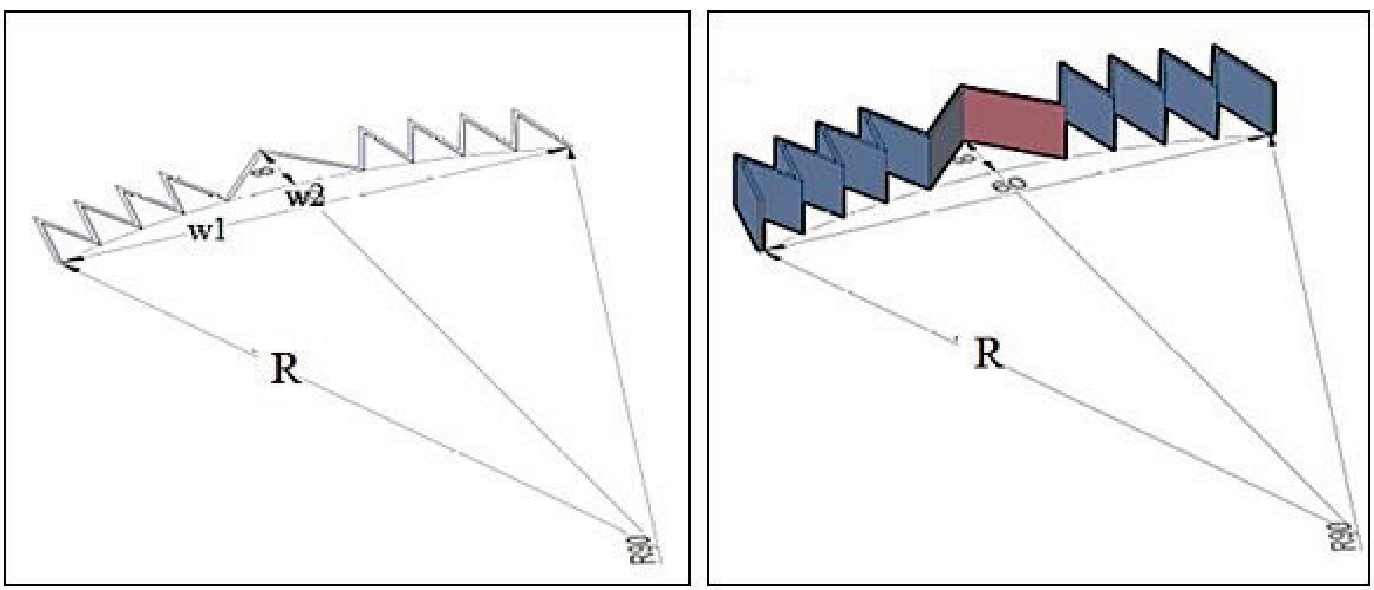

Figure 3. Plan and 3D view of arched asymmetry triangular labyrinth weir.

2026, Instituto Mexicano de Tecnología del Agua.
Open Access bajo la licencia CC BY-NC-SA 4.0
(https://creativecommons.org/licenses/by-nc-sa/4.0/)

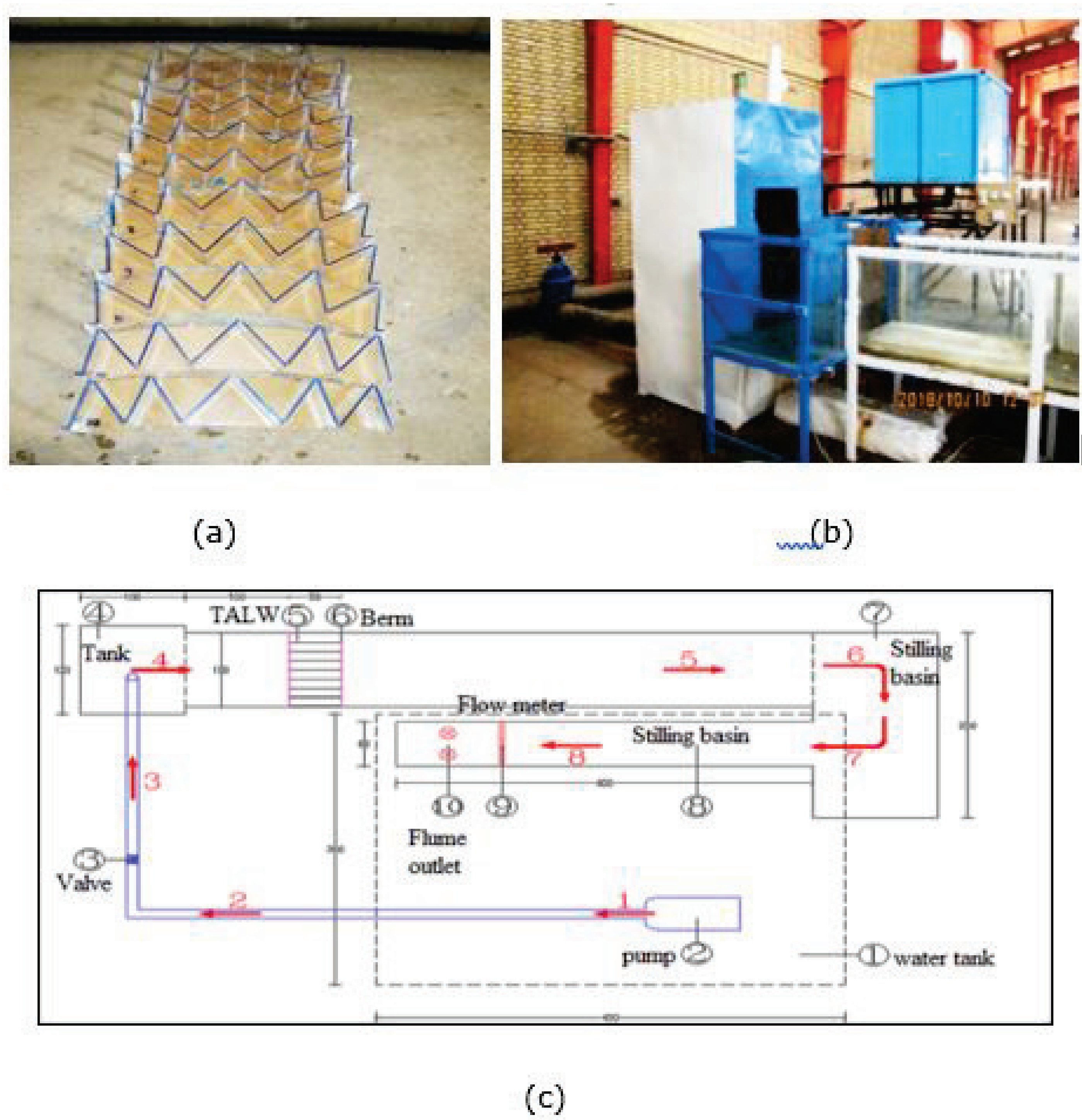

Figure 4. a) Physical model, b) experimental flume, and c) flume plan.

2026, Instituto Mexicano de Tecnología del Agua. Open Access bajo la licencia CC BY-NC-SA 4.0 (https://creativecommons.org/licenses/by-nc-sa/4.0/)

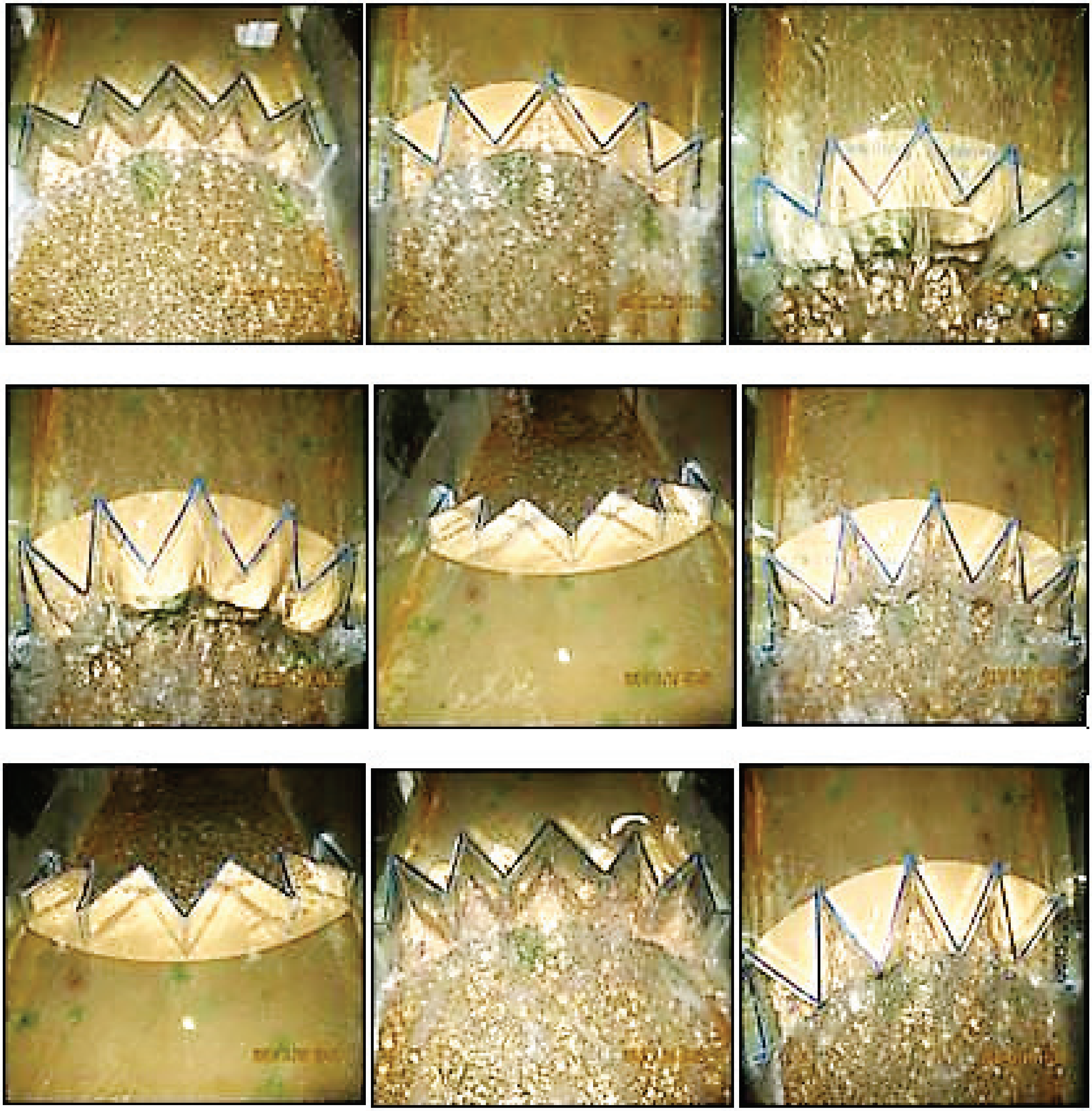

Figure 5. Triangle-arced asymmetry labyrinth weir during tests.

2026, Instituto Mexicano de Tecnología del Agua.
Open Access bajo la licencia CC BY-NC-SA 4.0
(https://creativecommons.org/licenses/by-nc-sa/4.0/)

Figure. 5 shows various types of physical weir models constructed with different designs and geometries.

Dimensional analysis

The value of Cd is a critical parameter influencing discharge of weirs. For labyrinth weirs, its value can be represented as a function of geometric and hydraulic parameters, expressed in the following form, Equation (1):

$$C_d = F(Q, Ht, W, P, L, B, w1, w2, t, R, \mu, \rho, \sigma, g, S, \varphi, N) \quad (1)$$

Referring to Figure 2:

Q = discharge

Ht = the total hydraulic head

W = the total width of the weir

P = the weir height

L = the weir length

B = the length of a weir cycle in the flow direction

w1 = the apex width for middle cycle

w2 = the apex width for side cycles

t = the weir thickness

R = the weir radius

μ = dynamic viscosity

ρ = density

2026, Instituto Mexicano de Tecnología del Agua.
Open Access bajo la licencia CC BY-NC-SA 4.0
(https://creativecommons.org/licenses/by-nc-sa/4.0/)

σ = surface tension of flow

g = acceleration of gravity

S = the bottom slope of flume

α = the weir arc angle

N = cycle number

To perform dimensional analysis, the parameters P, ρ, and Q were selected as repeating variables. The resulting dimensionless parameters were derived and are presented in Equation (2):

$$C_d = F\left(\frac{B}{P}, \frac{t}{P}, \frac{W}{P}, N, \frac{H_t}{P}, S, \frac{gP^5}{Q^2}, \frac{\mu P}{\rho Q}, \frac{w_1}{P}, \frac{w_2}{P}, \frac{\rho P^8}{\sigma Q^2}\right) \quad (2)$$

The quantities P, W, N, S, t, and D were excluded from the analysis due to their constancy in this study. Additionally, considering the turbulent nature of the flow and its sufficient depth, the Reynolds number ($\frac{\mu P}{\rho Q}$) and Weber number ($\frac{\rho P^8}{\sigma Q^2}$) were disregarded. It should be noted that the influence of gravitational acceleration ($\frac{gP^5}{Q^2}$), which is indicative of the Froude number, was incorporated through the dimensionless parameter ($\frac{H_t}{P}$). By combining $\frac{B}{P}$ and $\frac{w_1}{P}$, the dimensionless variable $\frac{B}{w_1}$ was derived. Similarly, combining ($\frac{w_1}{P}$) and ($\frac{w_2}{P}$) resulted in the dimensionless variable ($\frac{w_1}{w_2}$). These modifications led to the formulation of Equation (3) for Cd:

$$C_d = F\left(\frac{H_t}{P}, \frac{w_1}{w_2}, \frac{B}{w_1}, \frac{R}{w_1}, Fr\right) \quad (3)$$

2026, Instituto Mexicano de Tecnología del Agua.
Open Access bajo la licencia CC BY-NC-SA 4.0
(https://creativecommons.org/licenses/by-nc-sa/4.0/)

Table 1, Table 2, and Table 3 present the hydraulic and geometric parameter values utilized in the experimental investigations of this study, aimed at analyzing the influence of the asymmetrical triangular plan on the discharge coefficient of the labyrinth weir.

Table 1. Specifications of the performed tests.

R (degree)	**W1**	**W2**	**B**	$\frac{R}{W_1}$	$\frac{B}{W_1}$
45	18	10	13	2.5	0.72
45	18	10	11	2.5	0.61
45	18	10	9	2.5	0.5
45	16	10	13	2.8	0.81
45	16	10	11	2.8	0.68
45	16	10	9	2.8	0.56
45	14	10	13	3.2	0.92
45	14	10	11	3.2	0.78
45	14	10	9	3.2	0.64
45	reference	reference	reference	reference	reference
90	reference	reference	reference	reference	reference
90	18	10	9	5	0.5
135	reference	reference	reference	reference	reference
135	18	10	9	7.5	0.5

2026, Instituto Mexicano de Tecnología del Agua.
Open Access bajo la licencia CC BY-NC-SA 4.0
(https://creativecommons.org/licenses/by-nc-sa/4.0/)

Table 2. Geometrical and hydraulic characteristics of arced weir.

Arc angle (degree)	W (m)	P (m)	Lc (m)	T (mm)	Crest shape	No. of tests	$\frac{H_t}{P}$	Q (l/s)
45	0.58	0.1	0.65	6	Simple arc	12	0.21-0.95	4.17-50
90	0.58	0.1	0.60	6	Simple arc	12		
135	0.58	0.1	0.57	6	Simple arc	12		

Table 3. Geometrical and hydraulic characteristics of triangular-arced asymmetric labyrinth weir.

Q (l/s)	$\frac{H_t}{P}$	No. of tests	Lc (m)	P (m)	W (m)	Arc angle (degree)
3.5-40.5	0.125-0.8	12	1.2	0.1	0.58	45
			1.15		0.58	45
			1.15		0.58	45
			1.30		0.58	45
			1.30		0.58	45
			1.15		0.58	45
			1.45		0.58	45
			1.45		0.58	45
			1.45		0.58	45
			1.4		0.58	90
			1.4		0.58	135

2026, Instituto Mexicano de Tecnología del Agua.
Open Access bajo la licencia CC BY-NC-SA 4.0
(https://creativecommons.org/licenses/by-nc-sa/4.0/)

Results and discussion

Effect of Fr V.S Cd

Figure 6, Figure 7, Figure 8, Figure 9, and Figure 10 illustrate the variation of Cd against different values of $\frac{R}{w_1}$ and $\frac{B}{w_1}$. As observed, an increase in Fr leads to a corresponding increase in the hydraulic coefficient. This trend signifies that as the discharge increases, the weirs demonstrate a higher capacity for discharge. The optimal performance is achieved at a 90-degree angle. Table 4 summarizes the results, presenting the highest values of the hydraulic conductivity coefficient obtained in the experiments. According to Table 4, the highest hydraulic conductivity coefficient was observed at a Froude number of 1.64. This finding indicates that higher discharges result in increased discharge rates and a corresponding rise in the hydraulic conductivity coefficient. However, at high discharge discharges, turbulence and disturbances reduce the flow velocity, leading to a decrease in the hydraulic conductivity coefficient.

2026, Instituto Mexicano de Tecnología del Agua. Open Access bajo la licencia CC BY-NC-SA 4.0 (https://creativecommons.org/licenses/by-nc-sa/4.0/)
Tecnología y ciencias del agua, ISSN 2007-2422, 17(1), 314-348. DOI: 10.24850/j-tyca-2026-01-08

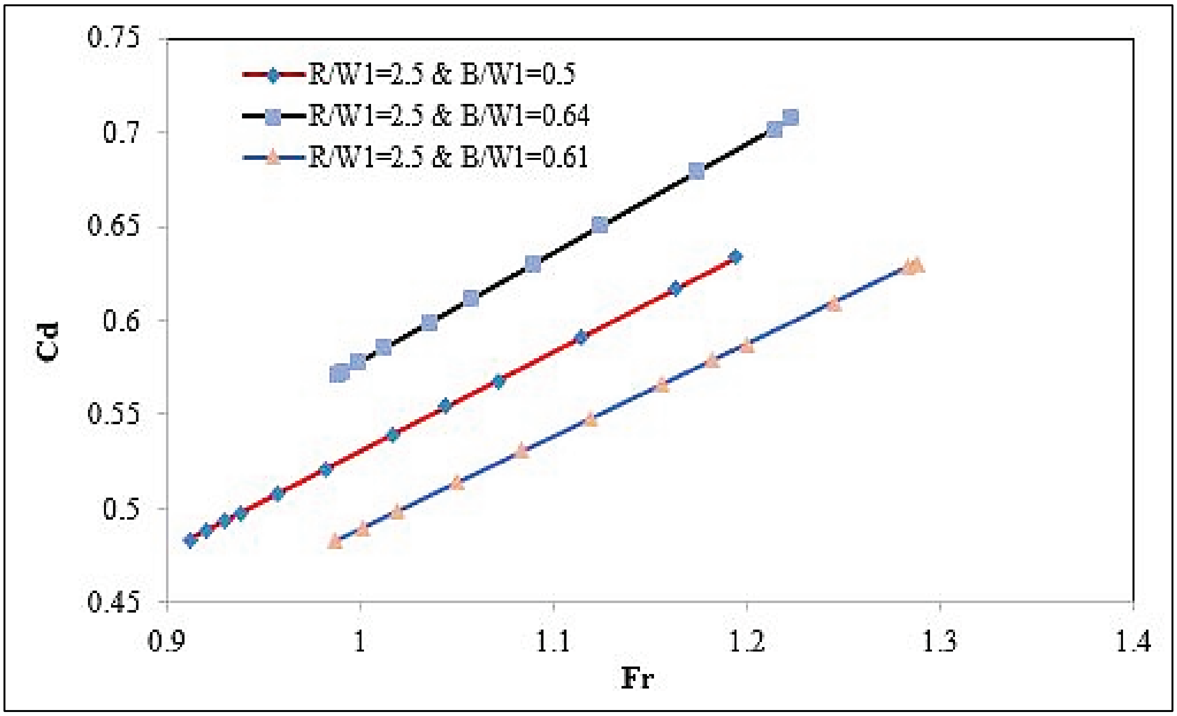

Figure 6. Effect of Fr V.S Cd for R/W1 = 2.5.

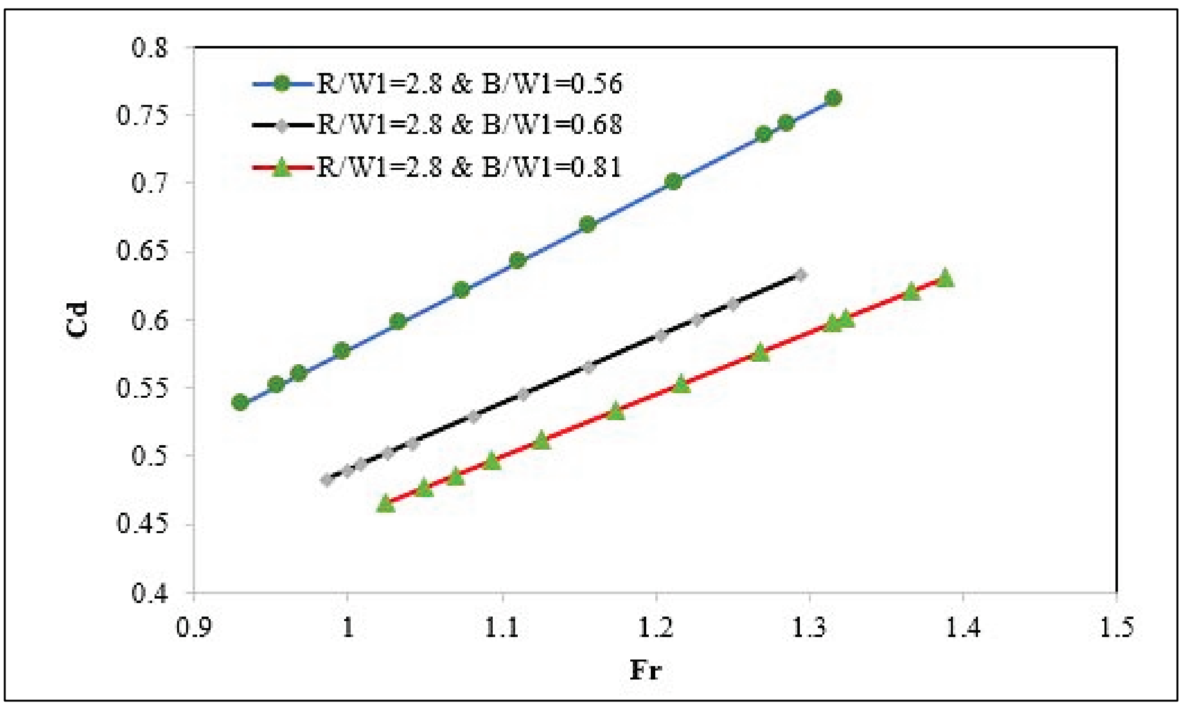

Figure 7. Effect of Fr V.S Cd For R/W1 = 2.8.

2026, Instituto Mexicano de Tecnología del Agua.
Open Access bajo la licencia CC BY-NC-SA 4.0
(https://creativecommons.org/licenses/by-nc-sa/4.0/)

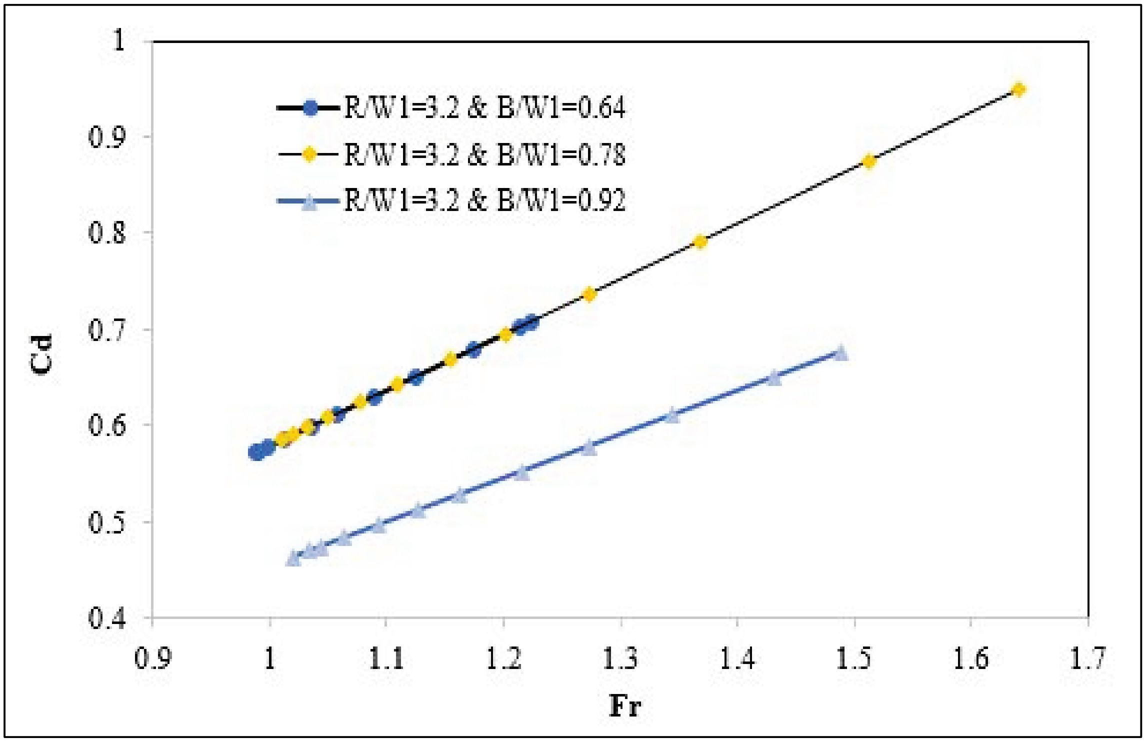

Figure 8. The effect of Fr V.S Cd For R/W1 = 3.2.

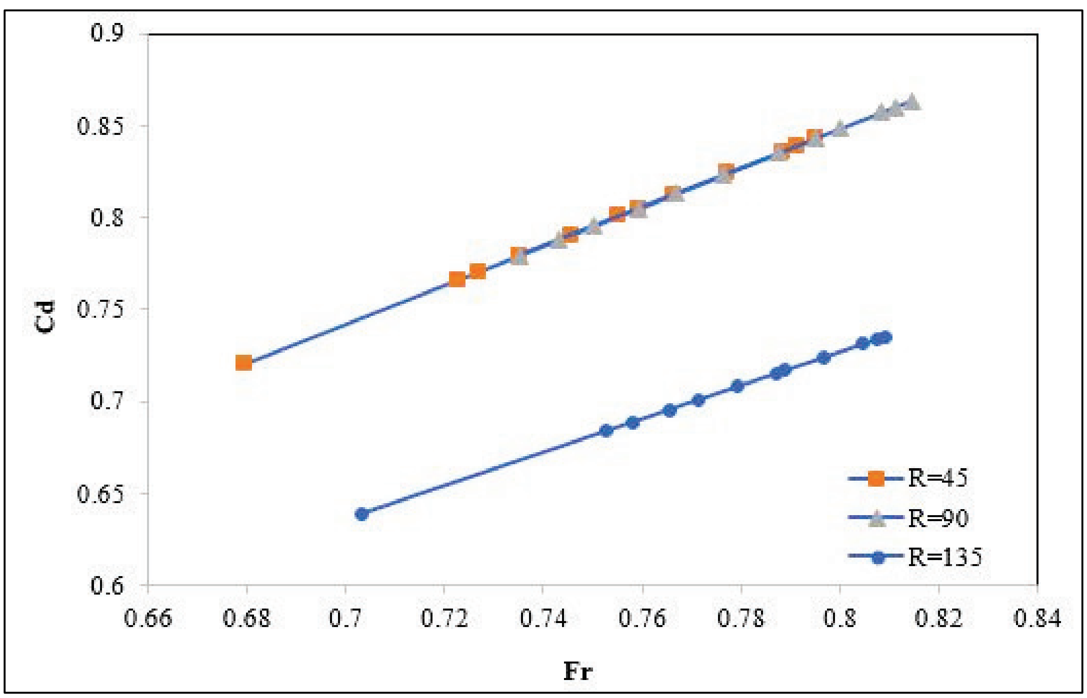

Figure 9. The effect of Fr V.S Cd for R.

2026, Instituto Mexicano de Tecnología del Agua.
Open Access bajo la licencia CC BY-NC-SA 4.0
(https://creativecommons.org/licenses/by-nc-sa/4.0/)

Tecnología y Ciencias del Agua

OPEN ACCESS

Check for updates

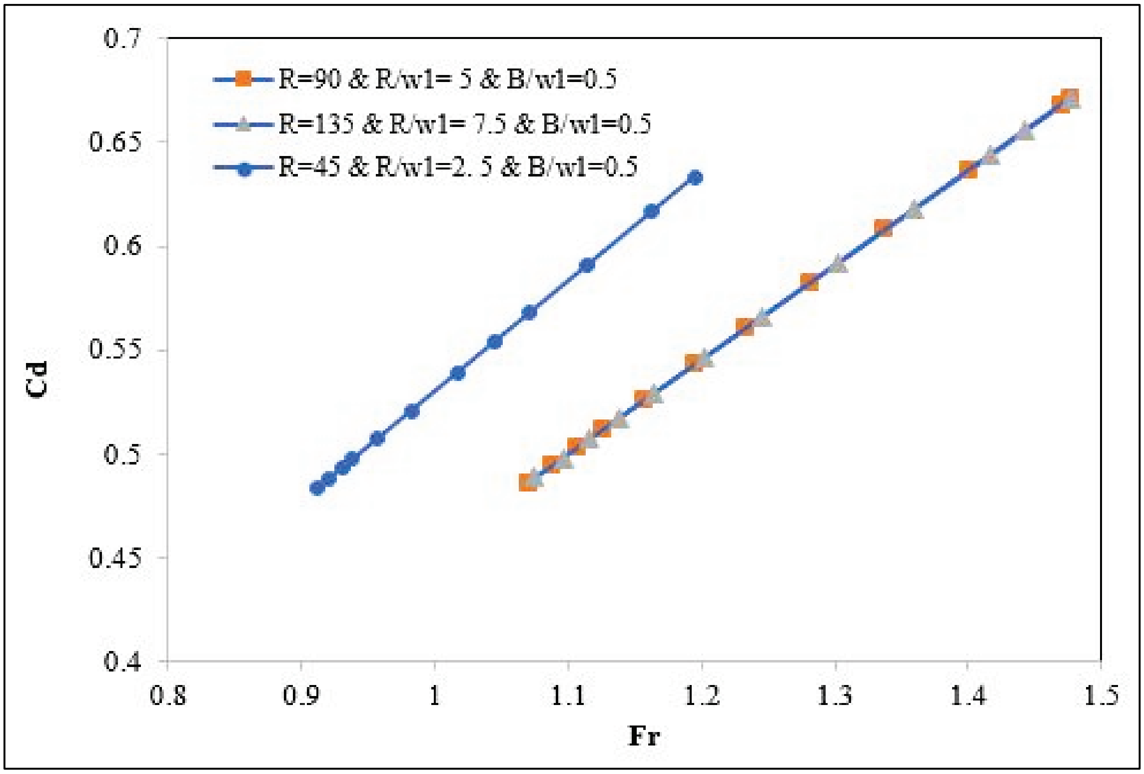

Figure 10. The effect of Fr V.S Cd for B/W1 = 0.5.

Table 4. The highest values of each model in Froude number.

Cd	Fr	R/W1	B/W1
0.633283	1.194495	2.5	0.5
0.761009	1.315795	2.8125	0.5625
0.707498	1.223272	3.214286	0.642857
0.630182	1.2877	2.5	0.611111
0.633517	1.294515	2.8125	0.6875
0.949667	1.641987	3.214286	0.785714
0.622585	1.370037	2.5	0.722222
0.630894	1.388321	2.8125	0.8125
0.676784	1.489305	3.214286	0.928571

2026, Instituto Mexicano de Tecnología del Agua.
Open Access bajo la licencia CC BY-NC-SA 4.0
(https://creativecommons.org/licenses/by-nc-sa/4.0/)

Q-Ht curves

This section examines the impact of weirs on the Q-Ht curve, illustrating the upstream hydraulic head at a constant Q. Figure 11, Figure 12, and Figure 13 present the variations of Q-Ht for different values of R/W1 and $\frac{B}{w_1}$.

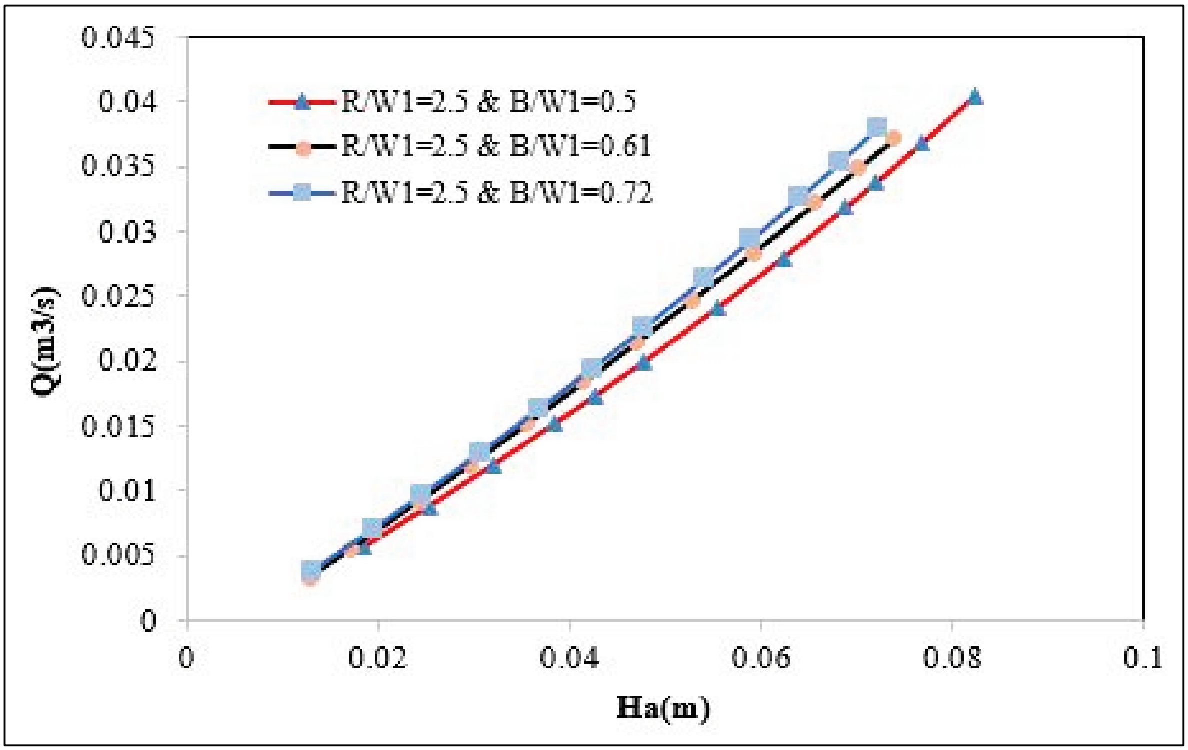

Figure 11. Q-Ht curve for R/W1 = 2.5.

2026, Instituto Mexicano de Tecnología del Agua.
Open Access bajo la licencia CC BY-NC-SA 4.0
(https://creativecommons.org/licenses/by-nc-sa/4.0/)
Tecnología y ciencias del agua, ISSN 2007-2422,
17(1), 314-348. DOI: 10.24850/j-tyca-2026-01-08

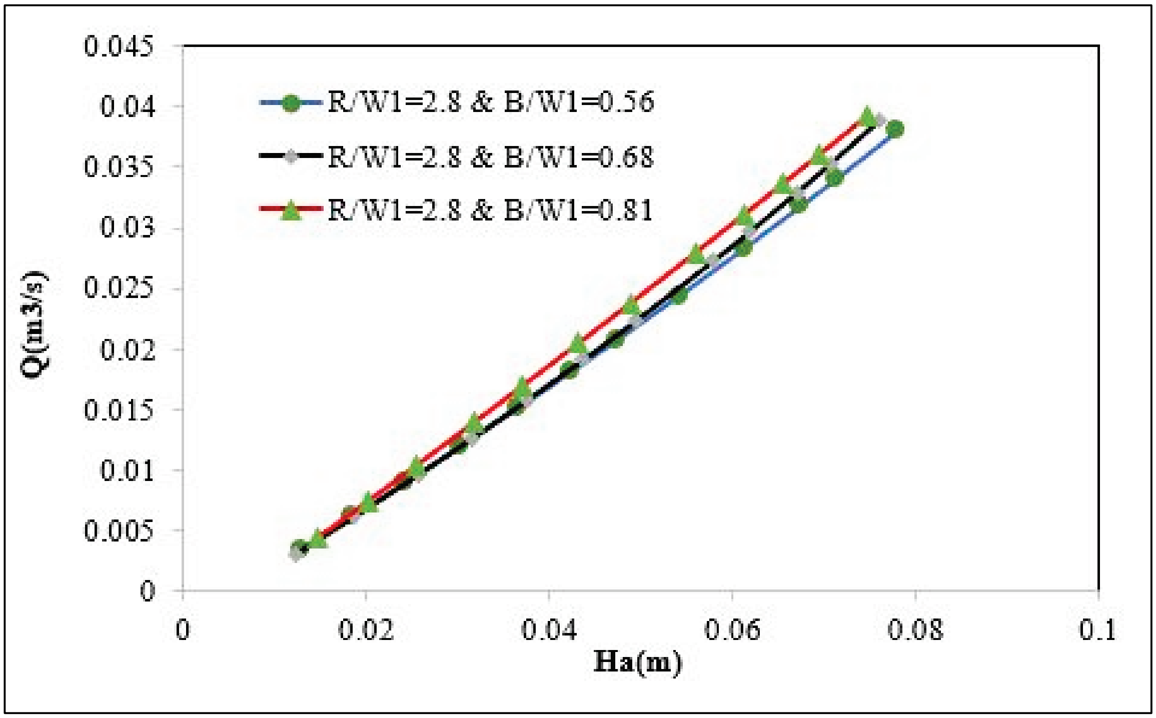

Figure 12. Q-Ht curve for R/W1 = 2.8.

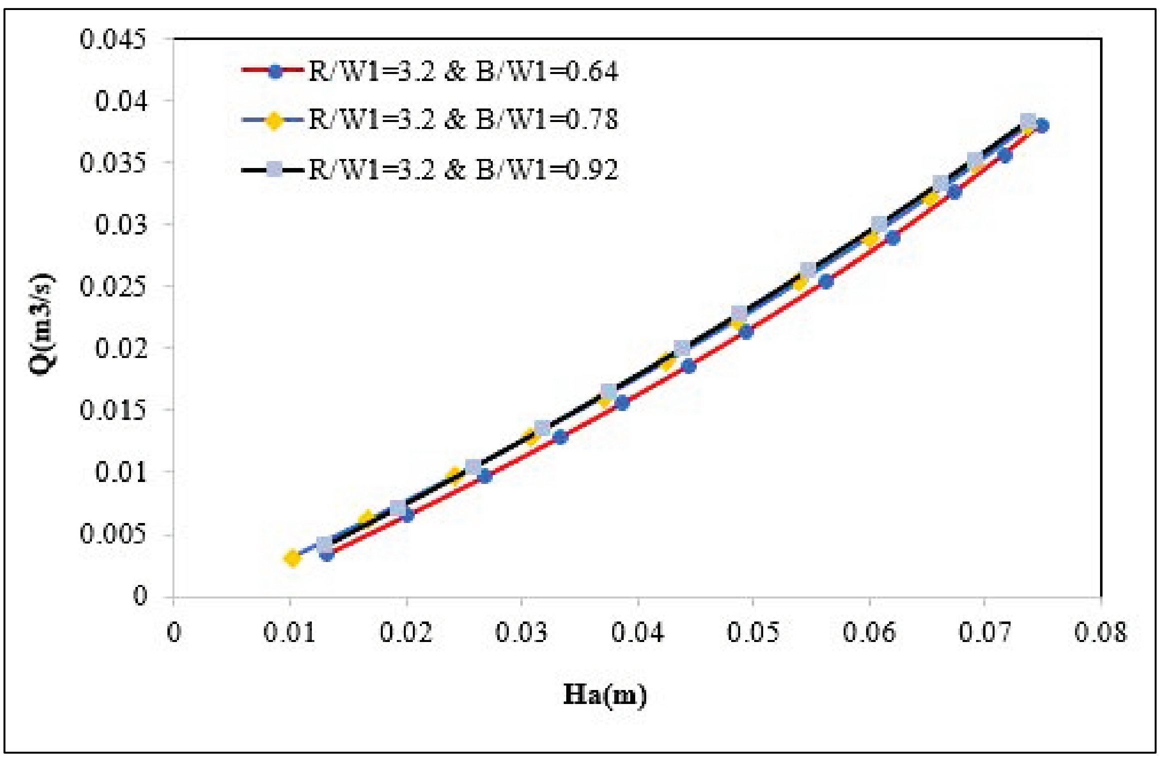

Figure 13. Q-Ht curve for R/W1 = 3.2.

2026, Instituto Mexicano de Tecnología del Agua. Open Access bajo la licencia CC BY-NC-SA 4.0 (https://creativecommons.org/licenses/by-nc-sa/4.0/)

As observed, for a constant discharge, a reduction in W1 results in an increased upstream hydraulic head. The decrease in W1 directs flow towards the weir outlet, increasing velocity along the weir while reducing lateral discharge. Consequently, the volume of flow passing through the weir rises. However, due to turbulence and flow disturbances at the weir's entrance, localized flow absorption occurs, which hinders discharge and raises the upstream hydraulic head. Notably, based on the slope of the discharge-hydraulic head curve under the tested conditions, it is plausible that at high hydraulic heads, reducing W1 could enhance the discharge capacity of the weir.

The effect of $\frac{H_t}{P}$ V.S Cd

Figure 14, Figure 15, Figure 16, Figure 17 and Figure 18 show the effect of $\frac{H_t}{P}$ on Cd for different values of $\frac{\mathbf{R}}{w_1}$ and $\frac{B}{w_1}$. In Figure 14 and Figure 15, the highest value of Cd occurs at $\frac{H_t}{P} = 0.2$. At values lower than this, Cd decreases due to adhesion at the weir and lack of aeration. Similarly, at higher values of $\frac{H_t}{P}$, the Cd decreases due to flow distortion. In Figure 16, the highest value Cd occurs at $\frac{H_t}{P} = 0.2$. At values lower than this, the Cd decreases due to adhesion at the weir and insufficient aeration. Similarly, at values greater than this, the coefficient decreases due to flow distortion. In Figure 17, the highest value of Cd occurs at $\frac{H_t}{P} = 0.1$. At values lower than this, Cd decreases due to adhesion at the weir and lack of aeration. Similarly, at values higher than this, the coefficient decreases due to flow distortion.

2026, Instituto Mexicano de Tecnología del Agua.
Open Access bajo la licencia CC BY-NC-SA 4.0
(https://creativecommons.org/licenses/by-nc-sa/4.0/)

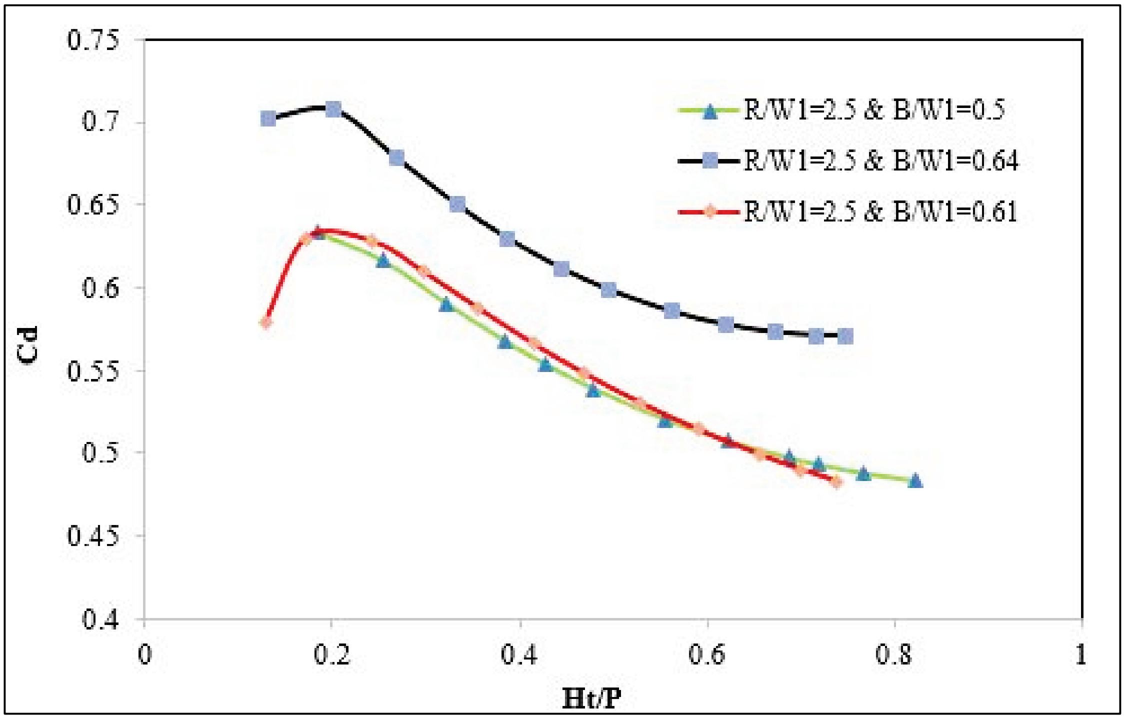

Figure 14. The effect of $\frac{H_t}{P}$ V.S Cd for R/W1 = 2.5.

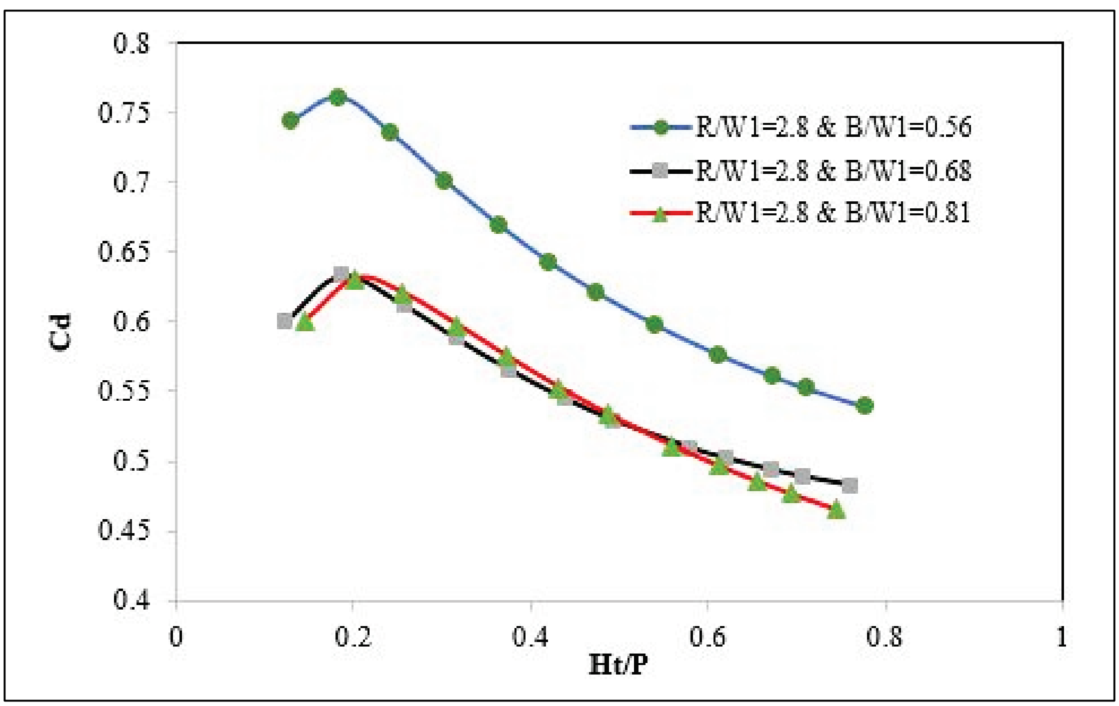

Figure 15. The effect of $\frac{H_t}{P}$ V.S Cd for R/W1 = 2.8.

2026, Instituto Mexicano de Tecnología del Agua.
Open Access bajo la licencia CC BY-NC-SA 4.0
(https://creativecommons.org/licenses/by-nc-sa/4.0/)

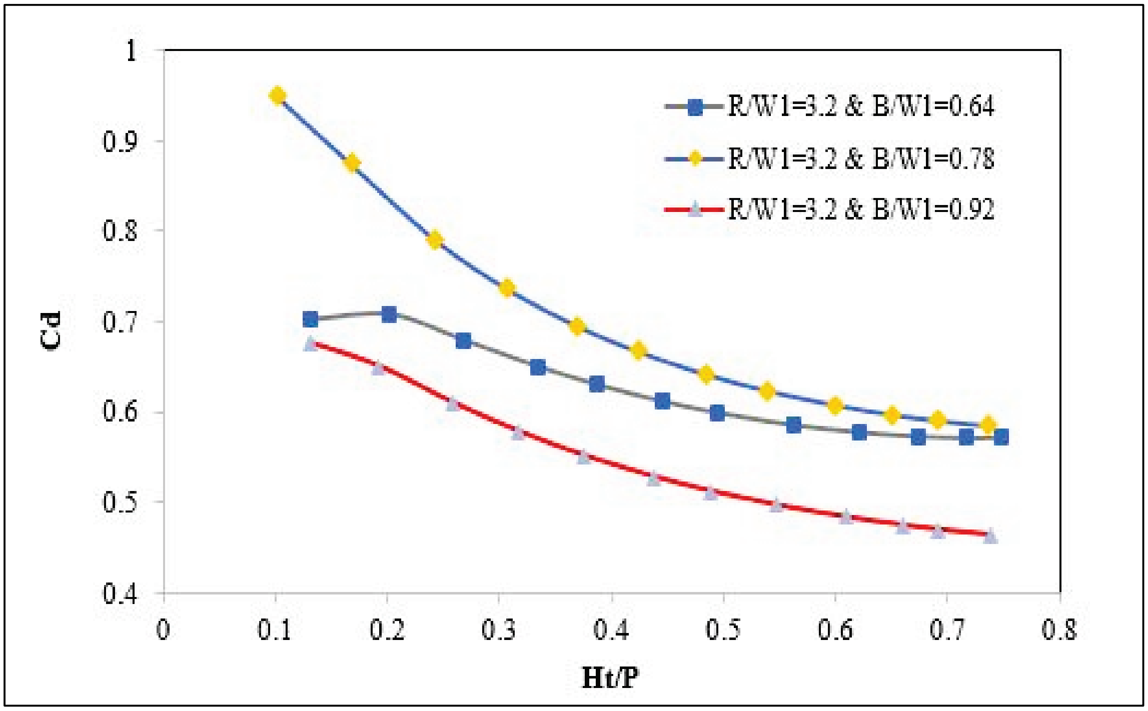

Figure 16. The effect of $\frac{H_t}{P}$ V.S Cd for R/W1 = 3.2.

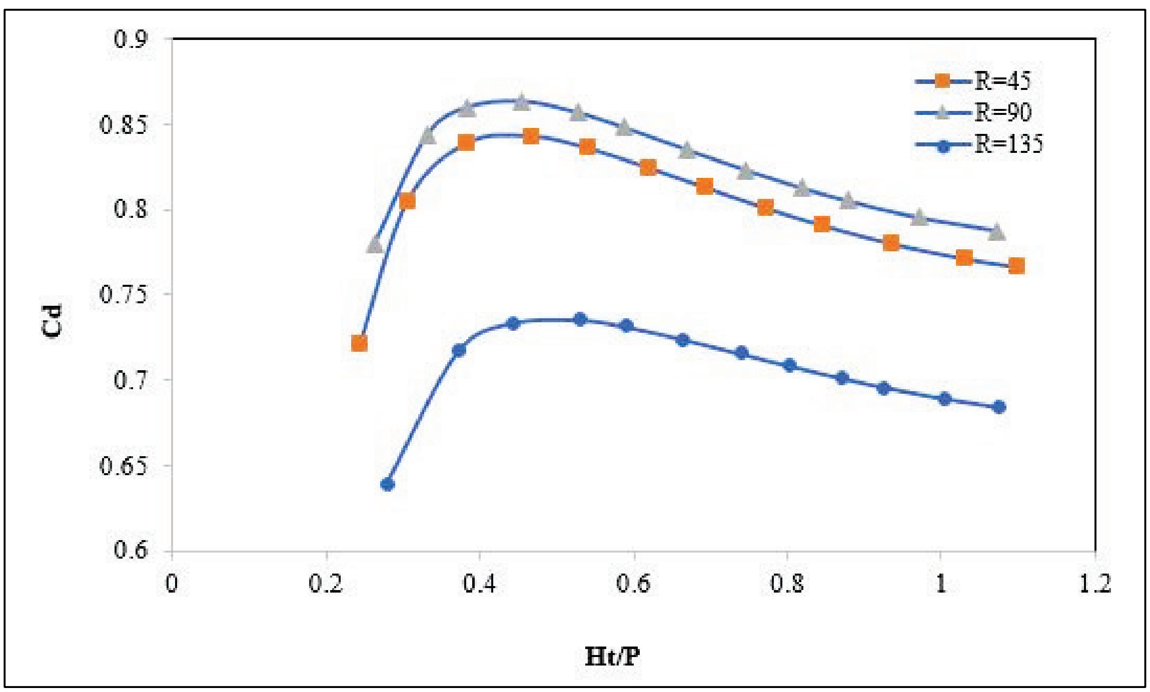

Figure 17. The effect of $\frac{H_t}{P}$ V.S Cd for R.

2026, Instituto Mexicano de Tecnología del Agua.
Open Access bajo la licencia CC BY-NC-SA 4.0
(https://creativecommons.org/licenses/by-nc-sa/4.0/)

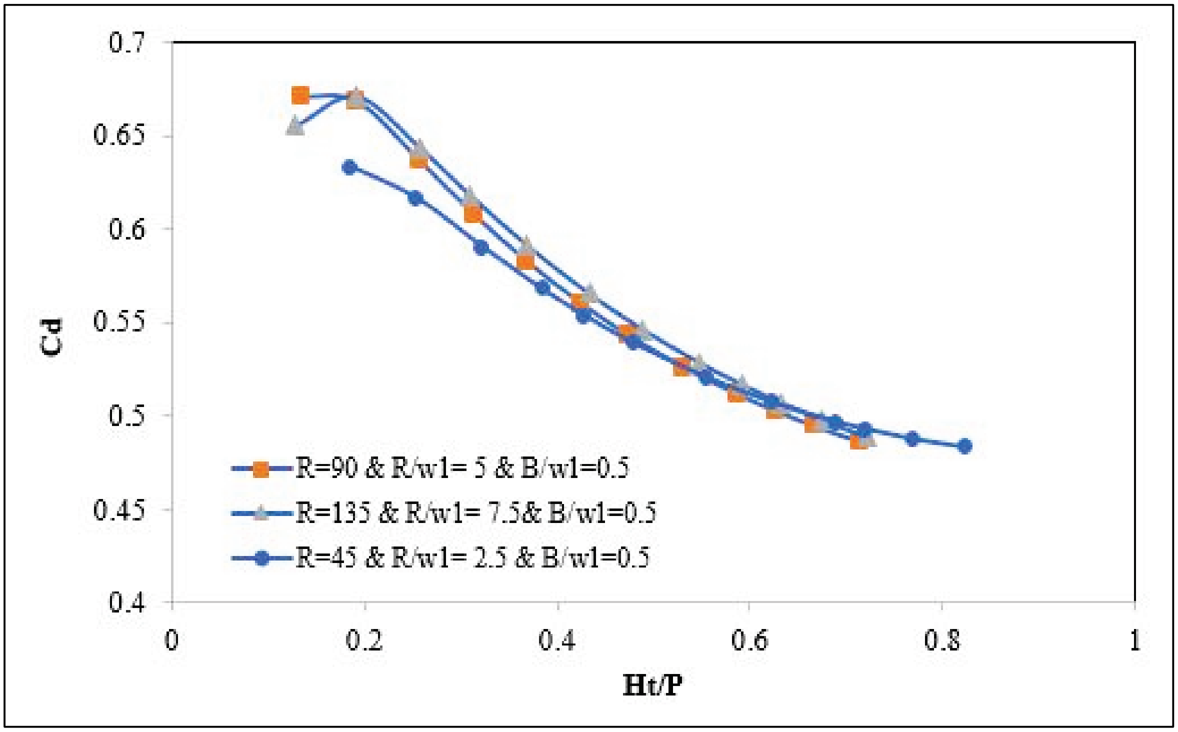

Figure 18. The effect of $\frac{H_t}{P}$ V.S Cd for B/W1 = 0.5.

In Figure 18, the highest value of Cd occurs at $\frac{H_t}{P} = 0.4$. At values lower than this, the value of Cd decreases due to adhesion at the weir and lack of aeration. Similarly, at values higher than this, the coefficient decreases due to flow distortion. Additionally, the optimal arc angle is 90 degrees. Based on the results of this diagram, it can be concluded that both increasing and decreasing the angle are not always beneficial. The best angle identified in this study is 90 degrees, as it provides the most efficient discharge. Angles of 45 degrees and 145 degrees are less effective due to the lower impact of the 45-degree angle and the high distortion associated with the 145-degree angle. Table 5 presents the values of the highest hydraulic conductivity coefficient distortion. Table 5 indicates the values of the highest hydraulic conductivity coefficient.

2026, Instituto Mexicano de Tecnología del Agua.
Open Access bajo la licencia CC BY-NC-SA 4.0
(https://creativecommons.org/licenses/by-nc-sa/4.0/)

Table 5. The highest values of each model in the Ht/P number.

Cd	Ht/P	R/W1	B/W1
0.633283	0.184507	2.5	0.5
0.761009	0.18403	2.8125	0.5625
0.707498	0.201867	3.214286	0.642857
0.630182	0.172715	2.5	0.611111
0.633517	0.186041	2.8125	0.6875
0.949667	0.101419	3.214286	0.785714
0.622585	0.195607	2.5	0.722222
0.630894	0.202242	2.8125	0.8125
0.676784	0.130494	3.214286	0.928571

As observed in Figure 14, Figure 15, Figure 16, Figure 17, and Figure 18, the discharge coefficient increases with the rise in upstream hydraulic head at low values of $\frac{H_d}{P}$ until it reaches a final head. However, beyond this point, as the discharge increases, the Cd gradually decreases due to flow interference and flow choking. This decrease occurs because the higher discharge leads to increased turbulence and choking at the weir, which diminishes its performance. This phenomenon continues until the weir reaches full absorption, after which the graph flattens, indicating that the weir becomes ineffective. As observed in the figures above, as the discharge increases, the nappe flow moves farther from the weir, causing obstructions in front of the weir. This results in a decrease in the Cd at the weir. Additionally, as the discharge increases, the formation of stacks in front of the weir intensifies, further reducing Cd. According to

2026, Instituto Mexicano de Tecnología del Agua. Open Access bajo la licencia CC BY-NC-SA 4.0 (https://creativecommons.org/licenses/by-nc-sa/4.0/)

the results of this study, increasing the angle of the weir head enhances the weir's efficiency.

Regarding changes in Froude number, it should be noted that as Froude number increases, the discharge coefficient increases. In other words, there is a direct relationship between Froude number and discharge coefficient.

Comparison of the results of the present study with other research

To compare the results of the present study with other research, labyrinth weirs with the characteristics of R = 45 deg (present study) and triangular labyrinth weirs with R = 37.5 deg (Monjezi *et al*., 2018) were used. Therefore, in Figure 3, the Research Results are presented for present study in comparison with Monjezi *et al*. (2018).

According to Figure 19, higher values in the range of 0.65 to 0.9 for Cd indicate better performance compared to the study by Monjezi *et al*. (2018). Lower values in the range of 0.4 to 0.7 for Cd reflect reduced efficiency with a decrease in the bend angle (R). The difference of approximately 0.1 to 0.2 in Cd values between the two studies may be attributed to variations in experimental design or boundary conditions. Furthermore, it can be stated that increasing the angle from 37.5 to 45 degrees leads to improved hydraulic performance and an increase in the discharge coefficient.

2026, Instituto Mexicano de Tecnología del Agua.
Open Access bajo la licencia CC BY-NC-SA 4.0
(https://creativecommons.org/licenses/by-nc-sa/4.0/)

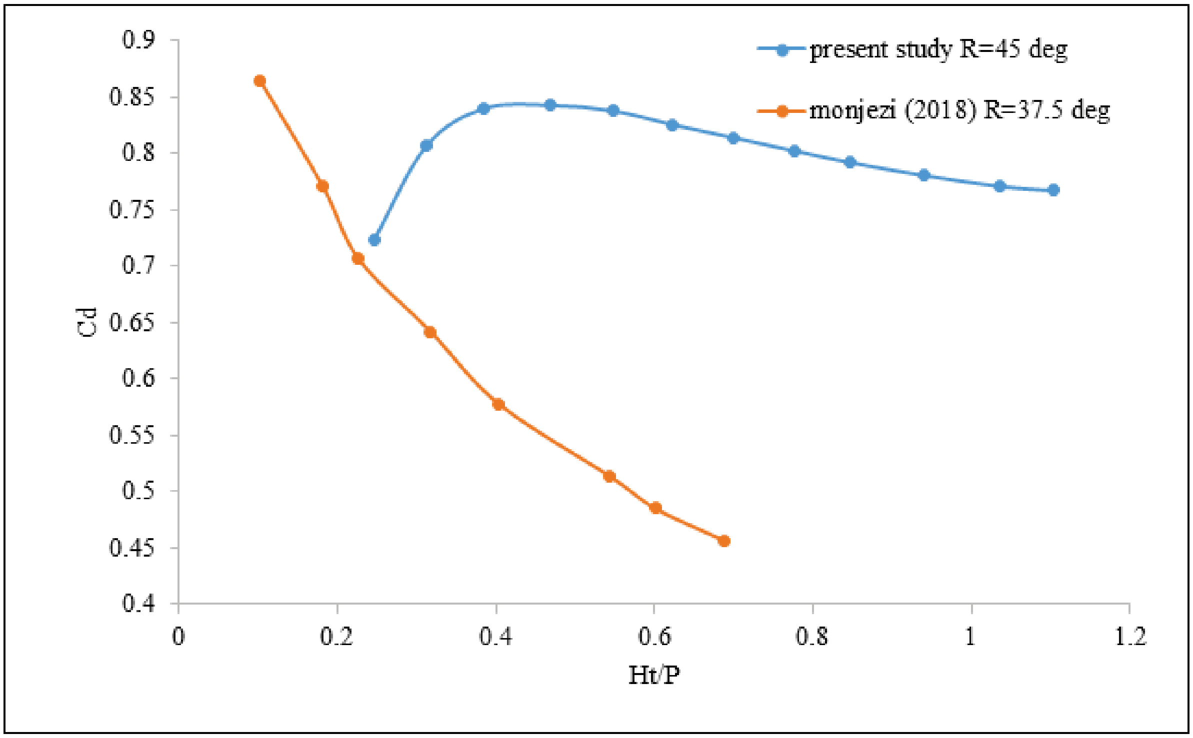

Figure 19. The effect of $\frac{H_t}{P}$ V.S Cd.

Conclusions

This research conducted an in-depth experimental investigation into the hydraulic performance of triangular-arced asymmetric labyrinth weirs under varying geometrical and hydraulic conditions. The primary aim was to analyze the effects of intermediate cycle modifications, arc angles, and other geometric parameters on Cd, a key indicator of hydraulic efficiency. The findings contribute valuable insights into optimizing labyrinth weir designs for flood control and other hydraulic applications. Labyrinth weirs are known for their capacity to handle high discharges under relatively low hydraulic heads, making them an efficient solution for spillway designs in space-constrained settings. This study introduced a novel approach by focusing on asymmetric triangular plans and arced

2026, Instituto Mexicano de Tecnología del Agua.
Open Access bajo la licencia CC BY-NC-SA 4.0
(https://creativecommons.org/licenses/by-nc-sa/4.0/)

Tecnología y ciencias del agua, ISSN 2007-2422,
17(1), 314-348. DOI: 10.24850/j-tyca-2026-01-08

geometries, examining the impact of these modifications on the weir's hydraulic performance. The results highlight several key findings that underscore the advantages and limitations of these designs. The arc angle emerged as a critical parameter influencing discharge efficiency. Among the tested angles (45°, 90° and 135°), the optimal performance was achieved at 90°. This angle provided the highest Cd, balancing flow stability, aeration, and reduced turbulence. Angles smaller than 90° limited flow interaction, reducing efficiency, while larger angles induced significant flow distortions, adversely affecting performance. Modifying the intermediate cycles by altering the apex widths (W1 and W2) and incorporating asymmetry improved hydraulic efficiency. Wider middle cycles enhanced discharge capacity by extending the effective flow path, thereby reducing localized turbulence. However, excessive widening resulted in flow concentration at specific points, diminishing overall effectiveness. Balancing these parameters is crucial for achieving optimal hydraulic performance. The study also examined the relationship between Cd and the Fr. Results showed an initial increase in Cd with rising Fr, attributed to enhanced hydraulic conductivity and flow momentum. However, at higher Fr values, turbulence and flow choking effects led to a decline in Cd. This underscores the importance of designing weirs for specific flow regimes to maximize efficiency. The Q-Ht curves revealed that as upstream hydraulic head increased, discharge capacity initially improved due to greater flow head. However, beyond a critical threshold, turbulence at the weir's entrance disrupted flow patterns, reducing efficiency. These findings highlight the need for careful consideration of hydraulic heads during the design phase to prevent performance degradation under high-flow conditions. The asymmetric triangular-arced weirs outperformed traditional labyrinth weirs in terms of discharge

2026, Instituto Mexicano de Tecnología del Agua. Open Access bajo la licencia CC BY-NC-SA 4.0 (https://creativecommons.org/licenses/by-nc-sa/4.0/)

efficiency. The combination of increased arc lengths and modified cycle geometries provided a more effective distribution of flow, minimizing energy losses and enhancing hydraulic conductivity. These improvements make asymmetric designs particularly suitable for applications requiring high discharge rates within limited spatial constraints.

References

Anderson, R. M., & Tullis, B. P. (2011). Comparison of piano key and rectangular labyrinth weir hydraulics. *Journal of Hydraulic Engineering*, 138(4), 358-361. DOI: https://doi.org/10.1061/(ASCE)HY.1943-7900.0000509

Aydin, M. C., Ulu, A. E., & Işık, E. (2024). Determination of effective flow behaviors on discharge performance of trapezoidal labyrinth weirs using numerical and physical models. *Modeling Earth Systems and Environment*, 10, 3763-3776. DOI: https://doi.org/10.1007/s40808-024-01996-3

Azimi, A. H., & Hakim, S. S. (2019). Hydraulics of flow over rectangular labyrinth weirs. *Irrigation Science*, 37(2), 183-193. DOI: https://doi.org/10.1007/s00271-018-0616-6

Ben-Said, M., Hafnaoui, M. A., & Madi, M. (2023). Numerical analysis of the influence of approach flow conditions on the efficiency of labyrinth weir. *Modeling Earth Systems and Environment*, 9(1), 41-51. DOI: https://doi.org/10.1007/s40808-022-01443-1

Cassidy, J. J., Gardner, C. A., & Peacock, R. T. (1985). Boardman labyrinth crest spillway. *Journal of Hydraulic Engineering*, 111(3), 398-416. DOI: https://doi.org/10.1061/(asce)0733-9429(1985)111:3(398)

2026, Instituto Mexicano de Tecnología del Agua. Open Access bajo la licencia CC BY-NC-SA 4.0 (https://creativecommons.org/licenses/by-nc-sa/4.0/)

Darvas, L. (1971). Discussion of performance and design of labyrinth weirs. *Journal of Hydraulic Engineering (ASCE)*, 97, 1246-1251. DOI: https://doi.org/10.1061/JYCEAJ.0003056

Dehghani, H. S., & Varaki, M. E. (2021). Experimental investigation of upstream sedimentation and downstream bed levels' effects on discharge coefficients of trapezoidal labyrinth weirs. *Arabian Journal of Geosciences*, 14, 1-16. DOI: https://doi.org/10.1007/s12517-021-08339-x

Dizabadi, S., Hakim, S. S., & Azimi, A. H. (2020). Discharge characteristics and structure of flow in labyrinth weirs with a downstream pool. *Flow Measurement and Instrumentation*, 71, 101683. DOI: https://doi.org/10.1016/j.flowmeasinst.2019.101683

Falvey, H. T. (2003). *Hydraulic design of labyrinth weirs*. Reston, USA: ASCE Press (American Society of Civil Engineers). DOI: https://doi.org/10.1061/9780784406311

Ghare, A. D., Mhaisalkar, V. A., & Porey, P. D. (2008). An approach to optimal design of trapezoidal labyrinth weirs. *World Applied Sciences Journal*, 3(6), 934-938.

Gupta, K. K., Kumar, S., & Ahmad, Z. (2015). Effect of weir height on flow performance of sharp crested rectangular–planform weir. *World Applied Sciences Journal*, 33(1), 168-175.

Hashem, T., Mohammed, A. Y., & Alfatlawi, T. J. (2024). Hydraulic characteristics of labyrinth sluice gate. *Flow Measurement and Instrumentation*, 96, 102556. DOI: https://doi.org/10.1016/j.flowmeasinst.2024.102556

2026, Instituto Mexicano de Tecnología del Agua. Open Access bajo la licencia CC BY-NC-SA 4.0 (https://creativecommons.org/licenses/by-nc-sa/4.0/)

Hay, N., & Taylor, G. (1970). Performance and design of labyrinth weirs. *Journal of Hydraulic Engineering*, 96(11), 2337-2357. DOI: https://doi.org/10.1061/JYCEAJ.0002766

Khode, B. V., Tembhurkar, A. R., Porey, P. D., & Ingle, R. N. (2011). Determination of crest coefficient for flow over trapezoidal labyrinth weir. *World Applied Sciences Journal*, 12(3), 324-329.

Kumar, S., Ahmad, Z., Mansoor, T., & Himanshu, S. K. (2012). Discharge characteristics of sharp crested weir of curved plan-form. *Research Journal of Engineering Sciences*, 1(4), 16-20.

Le, A. T., Hiramatsu, K., & Nishiyama, T. (2021). Hydraulic comparison between piano key weir and rectangular labyrinth weir. *Geomate Journal*, 20(82), 153-160. DOI: https://doi.org/10.21660/2021.82.j2106

Majedi-Asl, M., Fuladipanah, M., Arun, V., & Tripathi, R. P. (2022). Using data mining methods to improve discharge coefficient prediction in Piano Key and Labyrinth weirs. *Water Supply*, 22(2), 1964-1982. DOI: https://doi.org/10.2166/ws.2021.304

Masoudi, M. H., Yari, A., Sadeghian, J., & Norouzi, H. (2024). Experimental investigation of the discharge coefficient of the rectangular and trapezoidal labyrinth weirs considering variable congress lengths. *Modeling Earth Systems and Environment*, 10, 2819-2832. DOI: https://doi.org/10.1007/s40808-023-01925-w

Mattos-Villarroel, E. D., Ojeda-Bustamante, W., Díaz-Delgado, C., Salinas-Tapia, H., Flores-Velázquez, J., & Bautista-Capetillo, C. (2023). Methodological proposal for the hydraulic design of Labyrinth Weirs. *Water*, 15(4), 722. DOI: https://doi.org/10.3390/w15040722

2026, Instituto Mexicano de Tecnología del Agua. Open Access bajo la licencia CC BY-NC-SA 4.0 (https://creativecommons.org/licenses/by-nc-sa/4.0/)

Mirnaseri, M., & Emadi, A. (2014). Hydraulic performance of combined flow labyrinth weir-gate. *Advance in Agriculture and Biology*, 2, 54-60. DOI: https://doi.org/10.15192/pscp.aab.2014.1.1.article1

Monjezi, R., Heidarnejad, M., Masjedi, A., Purmohammadi, M. H., & Kamanbedast, A. (2018). Laboratory investigation of the Discharge Coefficient of flow in arced labyrinth weirs with triangular plans. *Flow Measurement and Instrumentation*, 64, 64-70. DOI: https://doi.org/10.1016/j.flowmeasinst.2018.10.011

Namazi, F. S. A., & Mozaffari, J. (2023). Investigation of labyrinth weirs discharge coefficient with the same length. *Flow Measurement and Instrumentation*, 94, 102468. DOI: https://doi.org/10.1016/j.flowmeasinst.2023.102468

Said, M. B., & Ouamane, A. (2024). Discharge capacity of an improved form of labyrinth weir. In: Kalinowska, M. B., Mrokowska, M. M., & Rowiński, P.M. (eds.). *Advances in hydraulic research. ISH 2023. GeoPlanet: Earth and planetary sciences*. Cham, Switzerland: Springer. DOI: https://doi.org/10.1007/978-3-031-56093-4_2

Seyedian, S. M., Haghiabi, A., & Parsaie, A. (2023). Reliable prediction of the discharge coefficient of triangular labyrinth weir based on soft computing techniques. *Flow Measurement and Instrumentation*, 92, 102403. DOI: https://doi.org/10.1016/j.flowmeasinst.2023.102403

Taylor, G. (1968). *The performance of labyrinth weirs* (Doctoral Thesis). University of Nottingham, UK.

2026, Instituto Mexicano de Tecnología del Agua. Open Access bajo la licencia CC BY-NC-SA 4.0 (https://creativecommons.org/licenses/by-nc-sa/4.0/)

Wang, F., Zheng, S., Ren, Y., Liu, W., & Wu, C. (2022). Application of hybrid neural network in discharge coefficient prediction of triangular labyrinth weir. *Flow Measurement and Instrumentation*, 83, 102108. DOI: https://doi.org/10.1016/j.flowmeasinst.2021.102108

Zhu, X., Si, J., Xie, W., & Tan, L. (2024). Discussion of "Discharge coefficient of symmetrical stepped and triangular labyrinth side weirs in a subcritical flow regime". *Journal of Irrigation and Drainage Engineering*, 150(3), 07024005. DOI: https://doi.org/10.1061/JIDEDH.IRENG-10230

2026, Instituto Mexicano de Tecnología del Agua.
Open Access bajo la licencia CC BY-NC-SA 4.0
(https://creativecommons.org/licenses/by-nc-sa/4.0/)